ChemElectroChem

Supporting Information

Spectroelectrochemical Behaviour of 1,4-Dimethoxypillar[5]arene (P5A) and its Monomer in Different Organic Solvents

Magdalena Z. Wiloch,* Ewelina Kuna, Sandra Kosiorek, Volodymyr Sashuk, and Martin Jönsson-Niedziółka*

SUPPORTING INFORMATION

Content

1. Additional electrochemical data

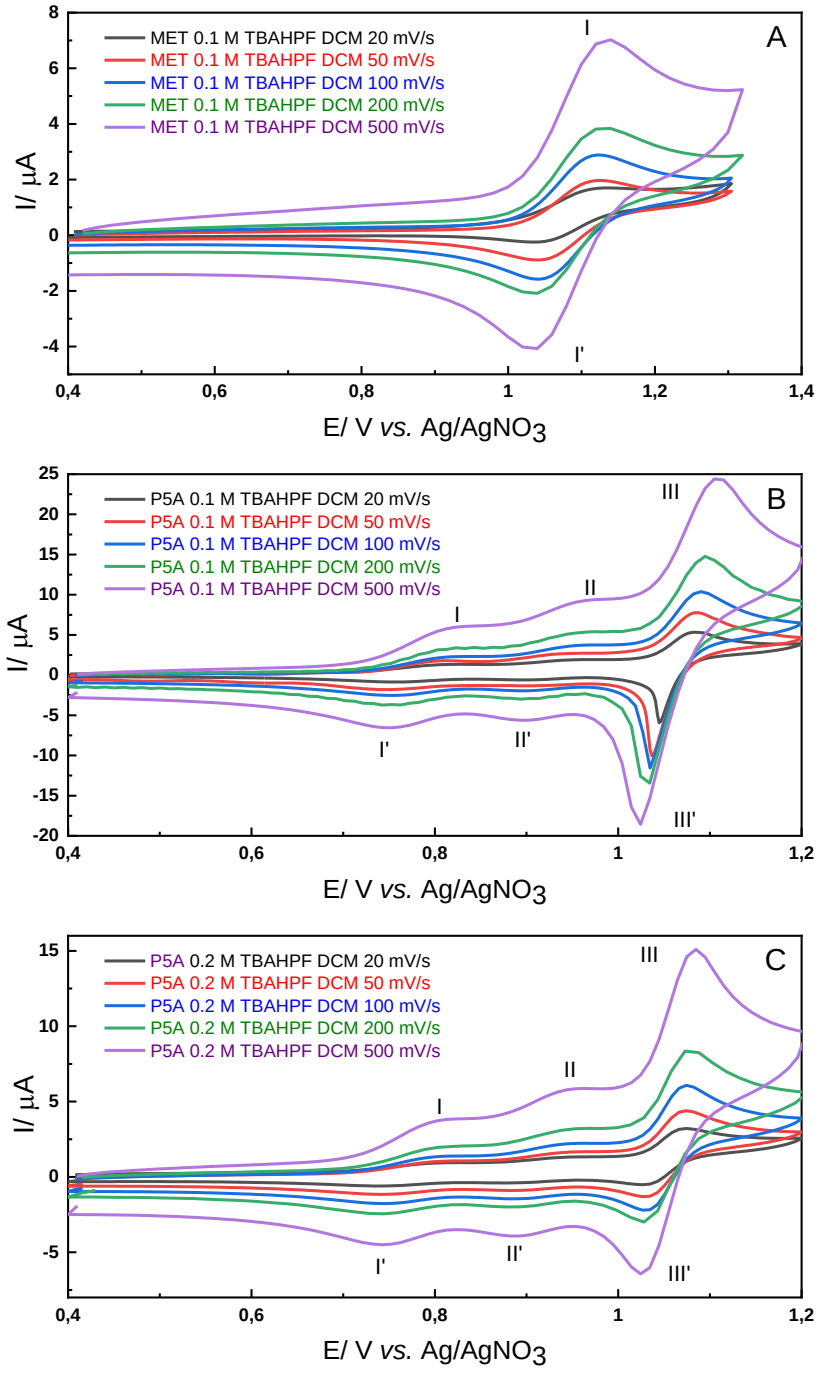

SI 1.1 Cyclic voltammograms on glassy carbon of (A) **0.1 mM** 1,4-dimethoxybenzene (**MET**) and (B, C) **0.1 mM** 1,4-dimethoxypillar[5]arene (**P5A**) in DCM containing (A,B) **0.1 M TBAHPF** or (C) **0.2 M** tetrabutylammonium hexafluorophosphate **(TBAHPF)** as supporting electrolyte, v = 100 mV/s. Scan rate dependence: *v* = 20, 50, 100, 200 and 500 mV/s.

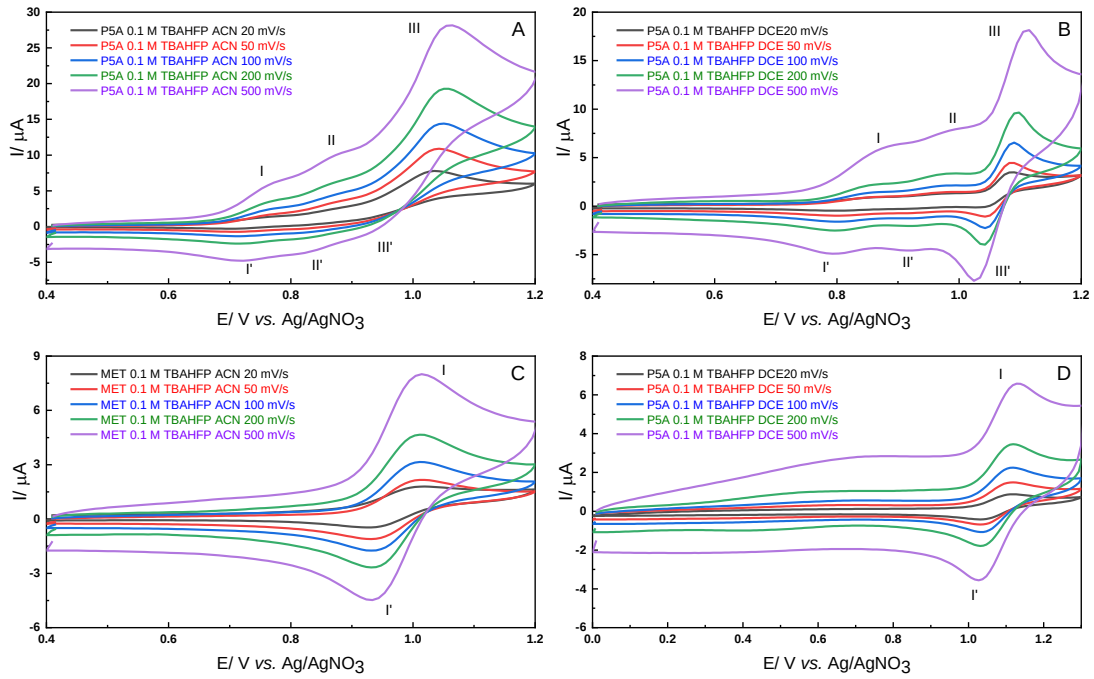

SI 1.2 Cyclic voltammograms on glassy carbon of (A,B) **0.1 mM P5A** or (*C*,*D*) **0.1 mM MET** in (A,C) ACN or (B,D) *DCE* containing **0.1 M TBAHPF** as supporting electrolyte as supporting electrolyte. Scan rate dependence: v = 20, 50, 100, 200 and 500 mV/s.

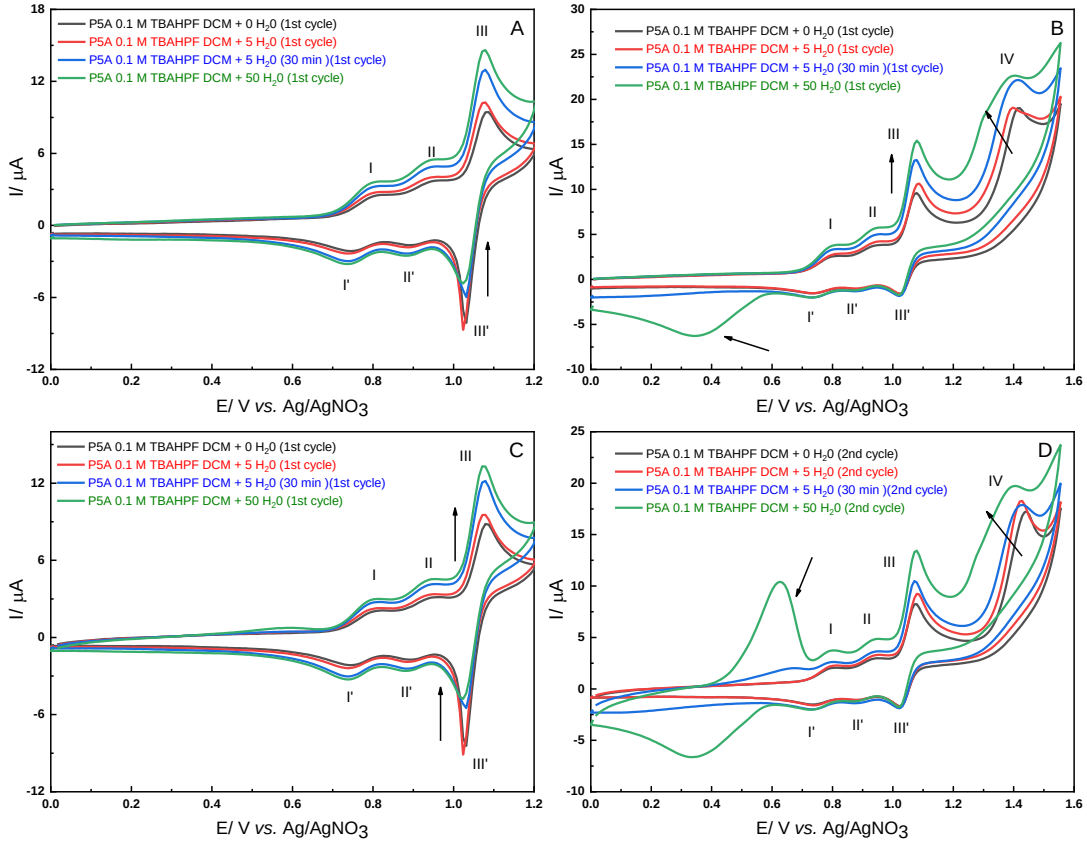

SI 1.3 Cyclic voltammograms on glassy carbon of **0.1 mM P5A in DCM** containing **0.1 M TBAHPF** as supporting electrolyte, *v* = 100 mV. Experiments performed: before adding water (black curves), and with water 0.1% (red curve), 0.1% after 30 minutes (blue curves) or 1% (green curves). First (2A, B) and second (2C, D) cycle shown.

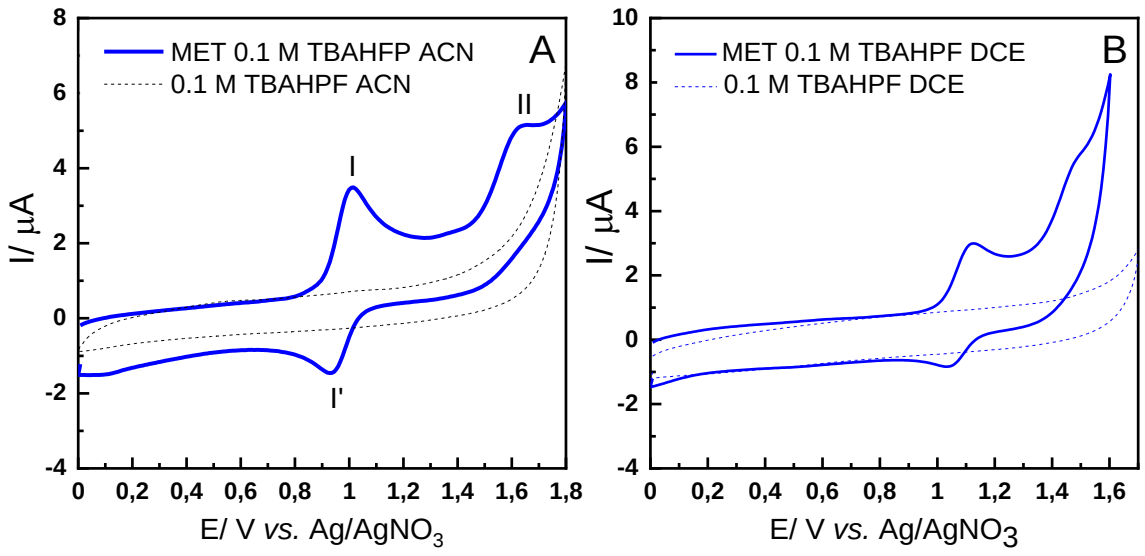

SI 1.4 Cyclic voltammograms on glassy carbon of **0.1 mM MET in** (A) **ACN** containing **0.1 M TBAHPF** as supporting electrolyte, (B) **DCE** containing **0.1 M TBAHPF** as supporting electrolyte. Scan rate dependence: *v* = 100 mV/s.

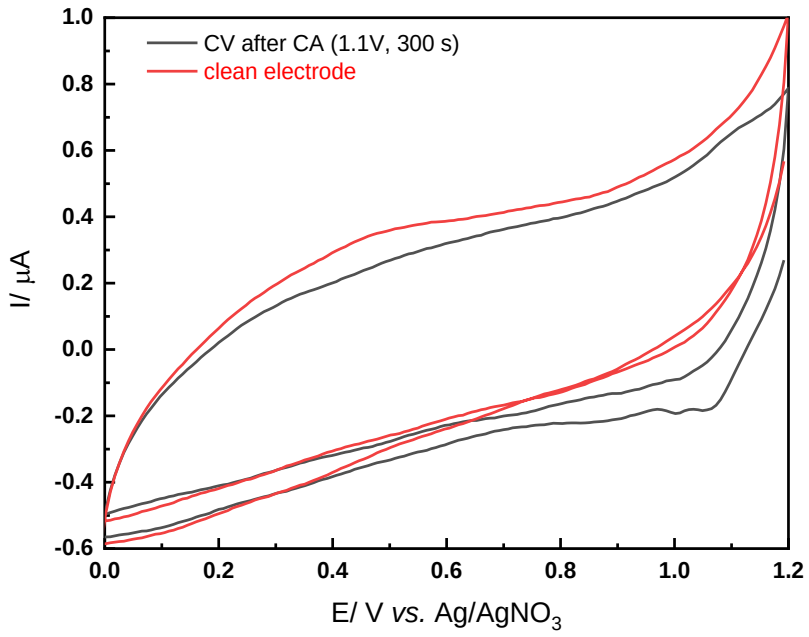

SI 1.5 Cyclic voltammograms **of 0.1 mM P5A** in on glassy carbon in **0.1 M TBAHPF DCM** ,v = 100 mV/s. Red curve recorded for clean electrode, black after CA (1.1V, 300 s).

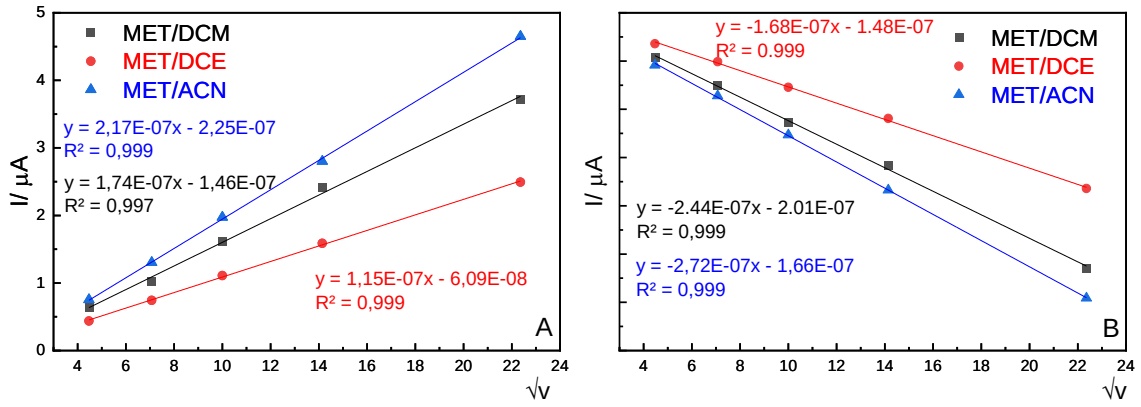

SI 1.6 Peak current vs the square root of the scan rate for **0.1 mM MET** dissolved in the solvents ACN, DCM, DCE containing **0.1M TBAHPF** as a supporting electrolyte. It is indicating that the MET redox process (oxidation (A) and reduction (B)) is controlled by diffusion in all solvents.

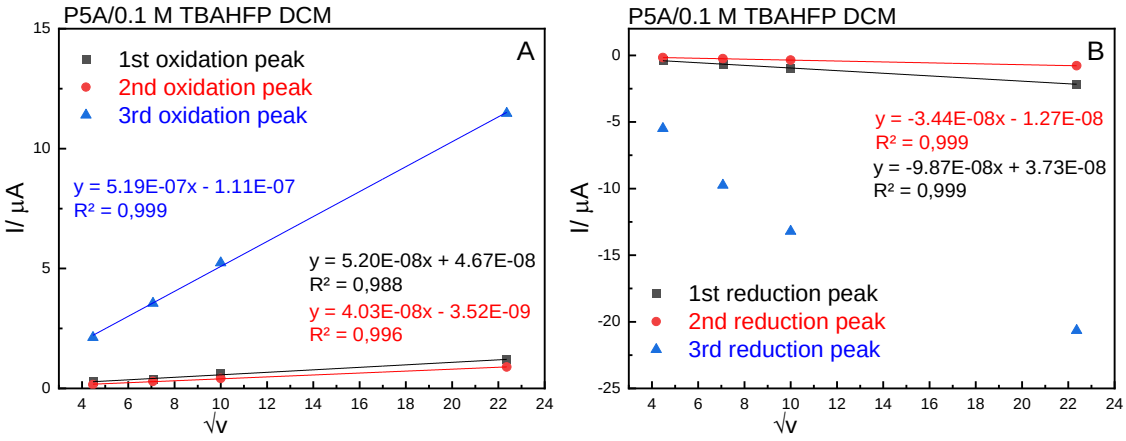

SI 1.7 Peaks current vs the square root of the scan rate for **0.1mM P5A** dissolved **in DCM** containing **0.1 M TBAHPF** as a supporting electrolyte. Indicating that the P5A redox process (oxidation -I, II, III and reduction I', II') are controlled by diffusion. There is no linear relationship for the third reduction peak, neither with the scan rate nor with the square root of the scanrate. This indicates a mixed mechanism.

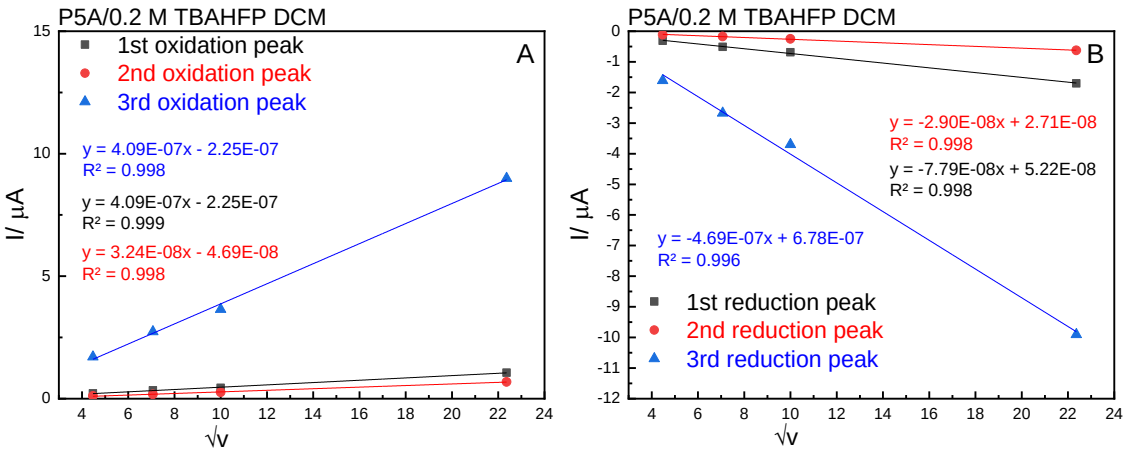

SI 1.8 Peaks current vs the square root of the scan rate for **0.1 mM P5A** dissolved **in DCM** containing **0.2 M TBAHPF** as a supporting electrolyte. It is indicating that the P5A redox process is limited by diffusion.

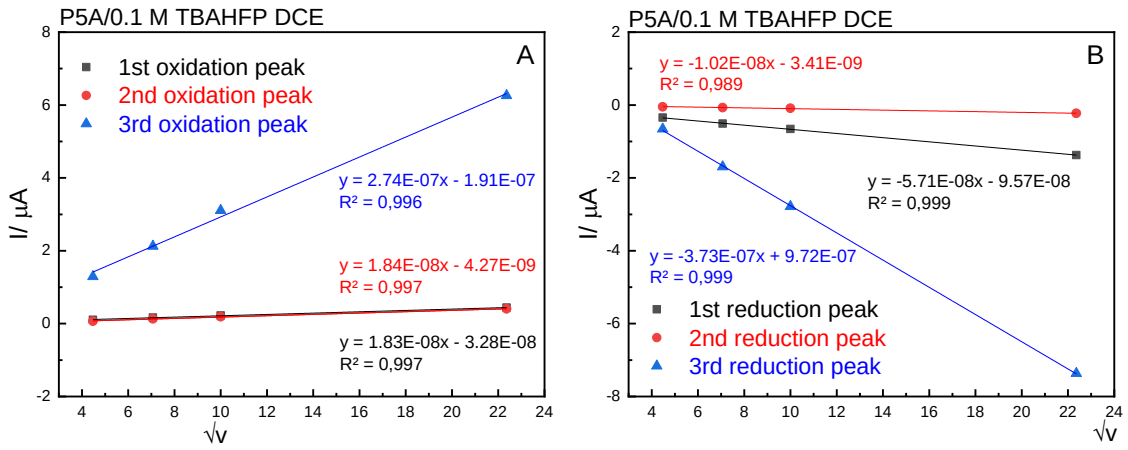

SI 1.9 Peaks current vs the square root of the scan rate for **0.1m M P5A** dissolved **in DCE** containing **0.1 M TBAHPF** as a supporting electrolyte. It is indicating that the P5A redox process is limited by diffusion.

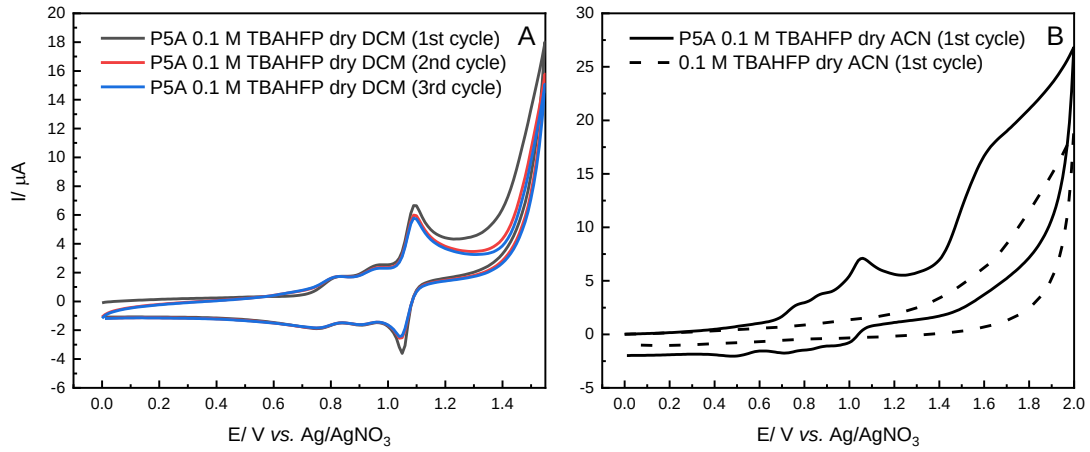

SI 1.10 Cyclic voltammograms on glassy carbon of **0.1 mM P5A in dry DCM** (A) or in dry CAN (B) containing **0.1 M TBAHPF** as supporting electrolyte, *v* = 100 mV. Experiments performed in glovebox.

2. Details on simulations

Simulations of the electrochemical response were performed using the software Comsol 5.6 with the Electrochemistry module. The simulations were performed using a 1D geometry with the electrode at one end and a constant concentration at the other end, sufficiently far away as to be well outside the depletion zone. The grid on the electrode side was refined until no difference in electrode current was seen. The electrode reaction was modelled using the Butler-Volmer equation with the exchange current density following the mass action law. [1] The electrode current density for each reaction is given by:

$$i = k_0 F n c_{ref,i} \left(\left(\frac{c_{Red,i}}{c_{ref,i}} \right)^{\alpha_{a,i}/n} \exp\left[\frac{\alpha_a F (E - E_{0,i})}{RT} \right] - \left(\frac{c_{Ox,i}}{c_{ref,i}} \right)^{\alpha_{c,i}/n} \exp\left[-\frac{\alpha_{c,i} F (E - E_{0,i})}{RT} \right] \right)$$

where k_0 is the reaction rate constant, c_{ref} the reference concentration, $c_{Red,i}$ and $c_{Ox,i}$ are the local concentrations of the reduced and oxidised forms of the redox probe, respectively, α_a the anodic transfer coefficient, $\alpha_c = n - \alpha_a$, F, R and T have their normal meanings. $E_{0,}$ is the equilibrium potential, and E is the electrode potential. The fourth, irreversible peak was modelled using a user-defined reaction, where the current density is given by $i = k_0 F n c_{Red,i} \exp\left[\frac{\alpha_a F (E - E_{0,i})}{RT} \right]$. Calculations were performed using both cyclic voltammetry with the same settings as in the experiments.

The voltammograms were fitted manually. The electrochemical parameters for the first reaction were fitted using the scan reversed before the second peak, and those values were carried over to the next voltage range. And so on. All the experimental voltammograms were background corrected before comparison with simulated data. The parameters used for the different reactions are found in table S1.

The simulations are very close to the experimental voltammograms for DCM and reasonably accurate for DCE (See Figure **SI 2.1**). No attempts were made to simulate the adsorption of the product from the third oxidation step. (See discussion in the main text). This should mainly account for the discrepancies in the fourth oxidation peak and the third reduction peak. For ACN, we failed to find suitable parameters (Figure **SI 2.2**) to fit the experimental data. The discrepancy is particularly large on the reverse scan. We also tried to fit that data using Digisim 3.0, but again failed to find a good fit. This indicates that the reactions in ACN, and to some extent in DCE, do not follow simple Butler-Volmer kinetics, which could be a sign of further interaction between the P5A and the solvent.

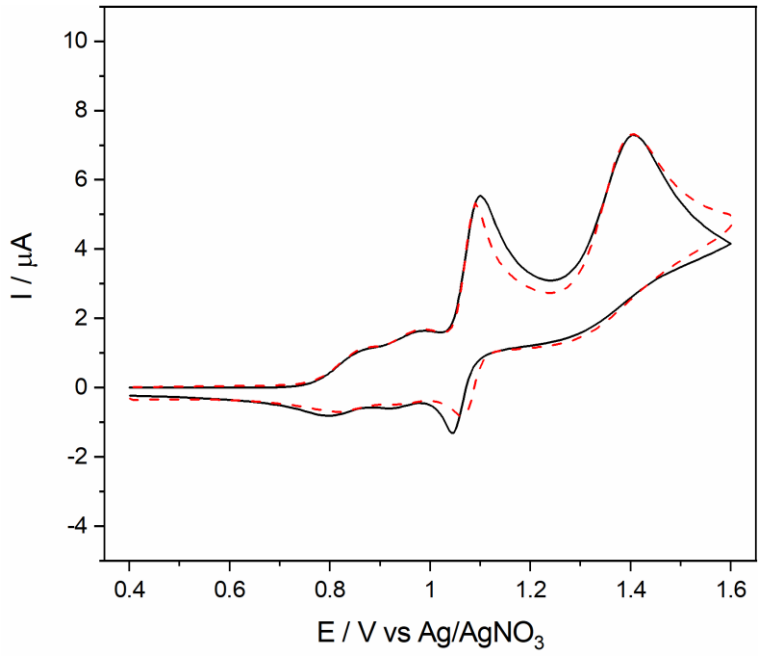

SI 2.1 Comparison of **0.1 mM P5A** cyclic voltammogram (dashed red line) with the simulated curve (full line) **in DCM** with **0.1 M TBAHPF**. Other conditions as in Fig 2.

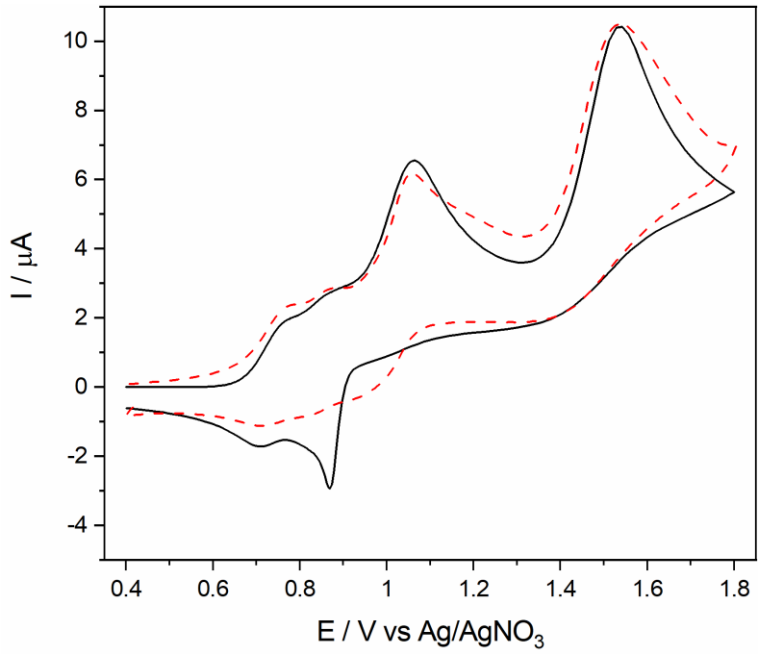

SI 2.2 Comparison of **0.1 mM P5A** cyclic voltammogram (dashed red line) with the simulated curve (full line) **in ACN** with **0.1 M TBAHPF**. Other conditions as in Fig 2.

Table S1 Parameters used in the Comsol simulations.

NAME	DCM 0.1M	DCM 0.2M	DCE	ACN	COMMENT
alpha1	0.52	0.52	0.30	0.40	Transfer coefficient reaction 1
alpha2	0.30	0.30	0.20	0.20	Transfer coefficient reaction 2
alpha3	0.66	0.61	1.05	0.60	Transfer coefficient reaction 3
alpha4	0.92	0.60	0.65	0.55	Transfer coefficient reaction 4
c0 [mM]	0.08	0.09	0.10	0.10	initial concentration
cref [mM]	1	1	1	1	reference concentration
D0 [cm^2/s]	8.20E-06	8.20E-06	4.30E-06	1.01E-05	diffusion coefficient
E01 [V]	0.773	0.778	0.832	0.733	Equilibrium potential reaction 1
E02 [V]	0.929	0.934	0.956	0.848	Equilibrium potential reaction 2
E03 [V]	1.052	1.061	1.068	0.915	Equilibrium potential reaction 3
E04 [V]	1.497	1.437	1.367	1.355	Equilibrium potential reaction 4
k01 [cm/s]	9.61E-03	6.40E-03	6.06E-03	1.31E-02	Rate coefficient reaction 1
k02 [cm/s]	1.06E-02	9.05E-03	5.78E-03	9.78E-03	Rate coefficient reaction 2
k03 [cm/s]	1.59E-02	1.37E-02	7.41E-03	9.00E-04	Rate coefficient reaction 3
k04 [cm/s]	7.00E-02	7.00E-03	2.50E-03	2.00E-04	Rate coefficient reaction 4

3. Additional spectroelectrochemical data

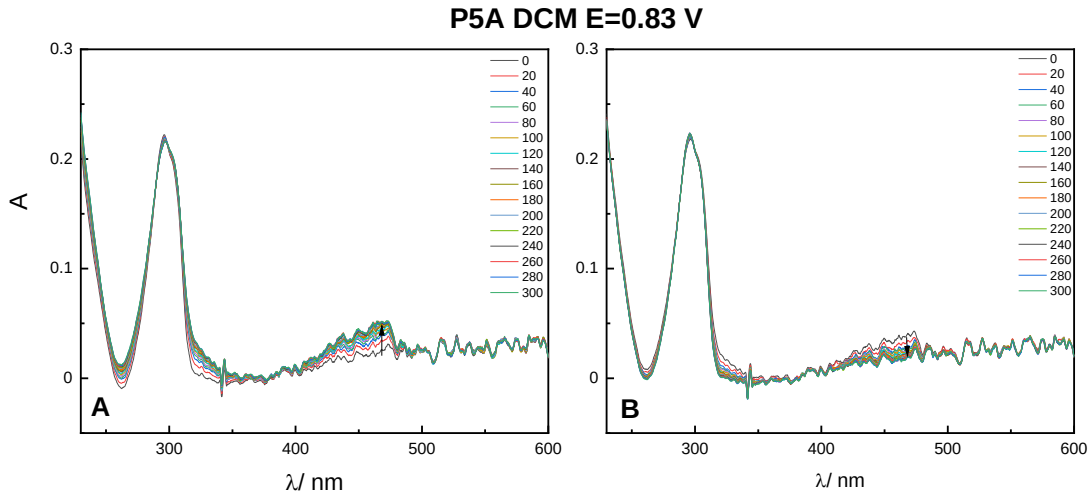

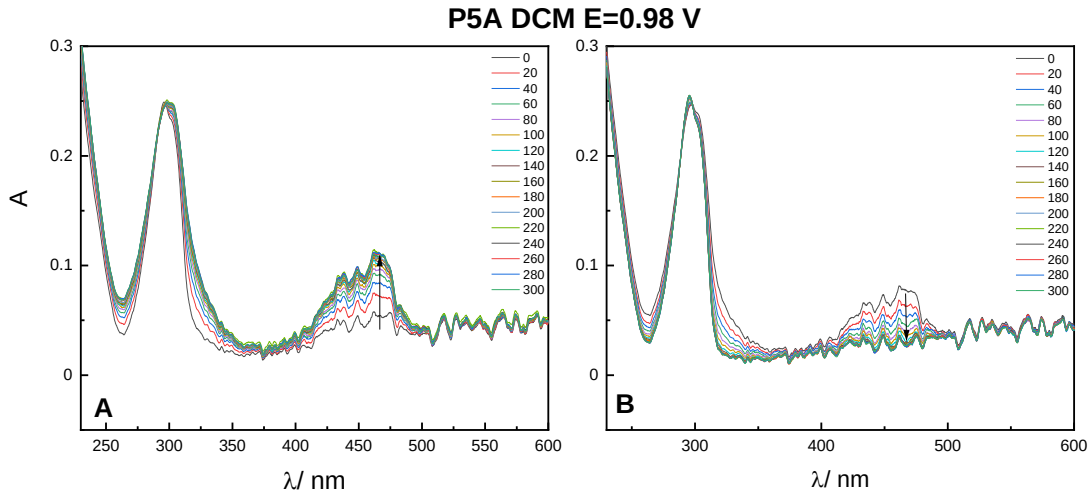

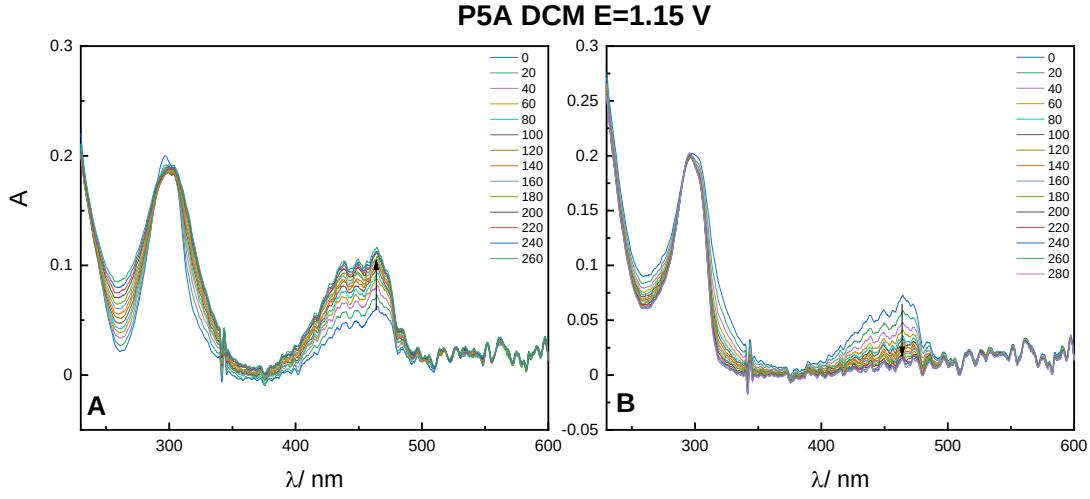

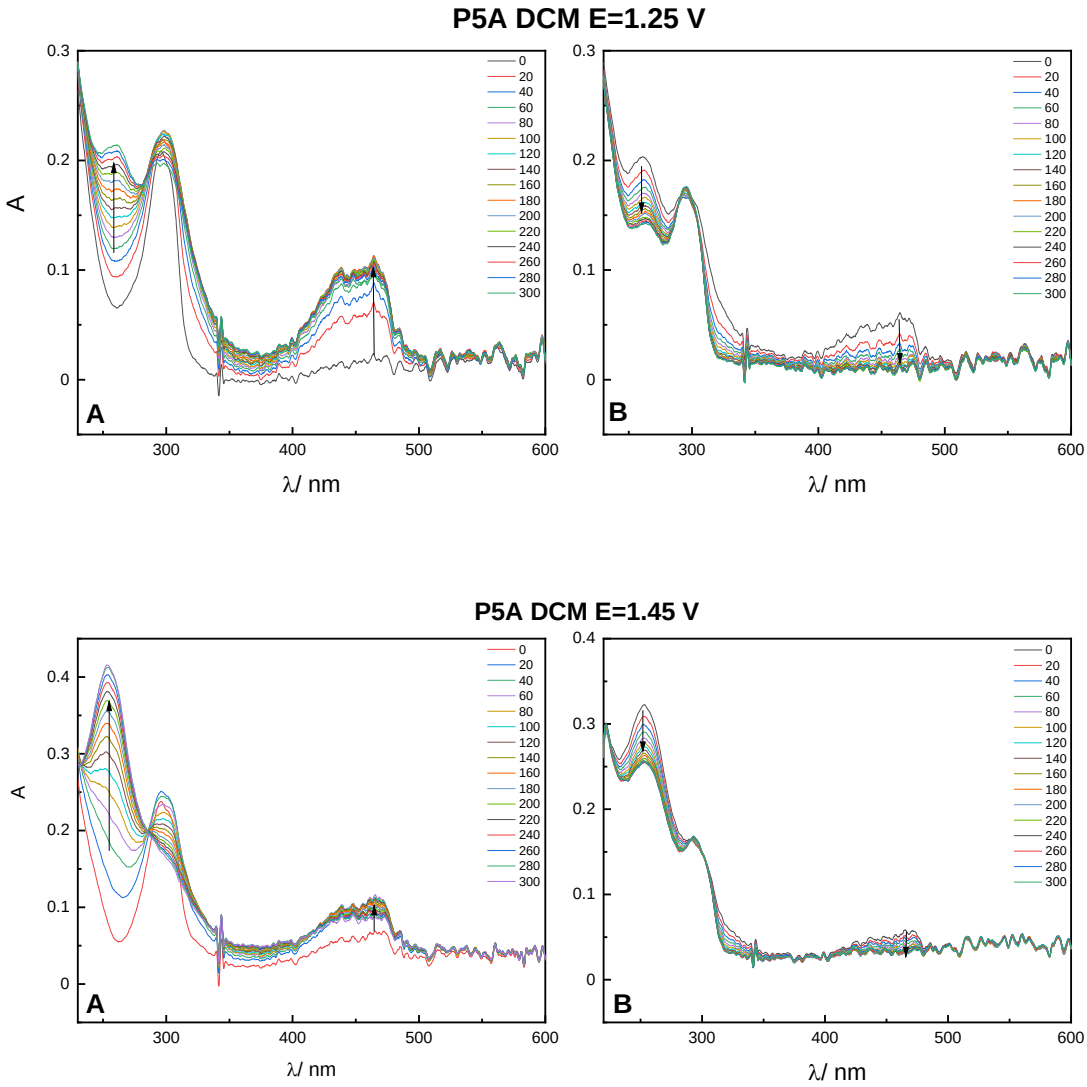

SI 3.1 The absorption spectra of **0.1 mM P5A** registered (A) at applied oxidative potential 0.83 V; 0.98 V; 1.15 V; 1.25 V and 1.45 V (B) and after measurements at the applied reductive potential of 0.2 V. Spectra recorded **in DCM** containing **0.1 M TBAHPF** at 22°C.

(A)

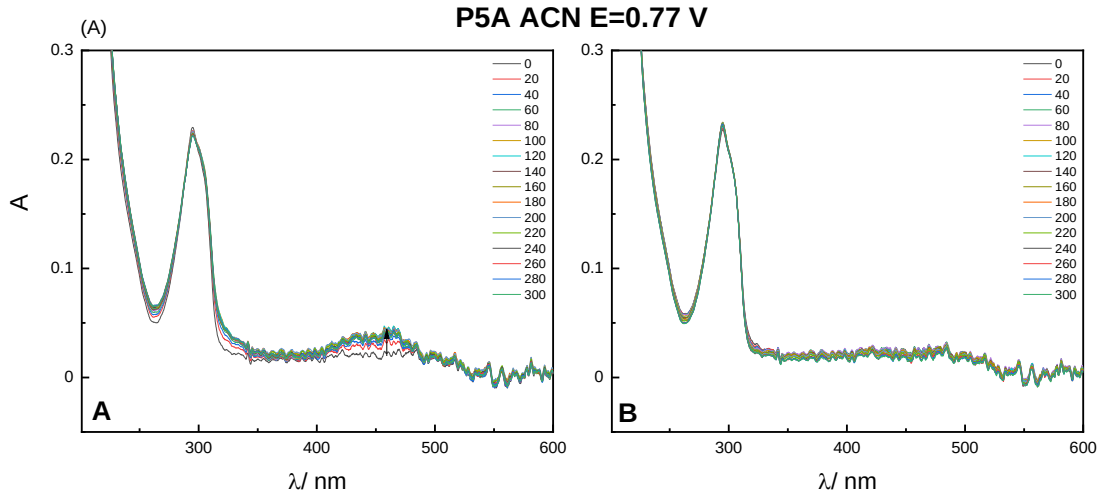
P5A ACN E=0.77 V
A
B
A
λ/ nm
0
20
40
60
80
100
120
140
160
180
200
220
240
260
280
300

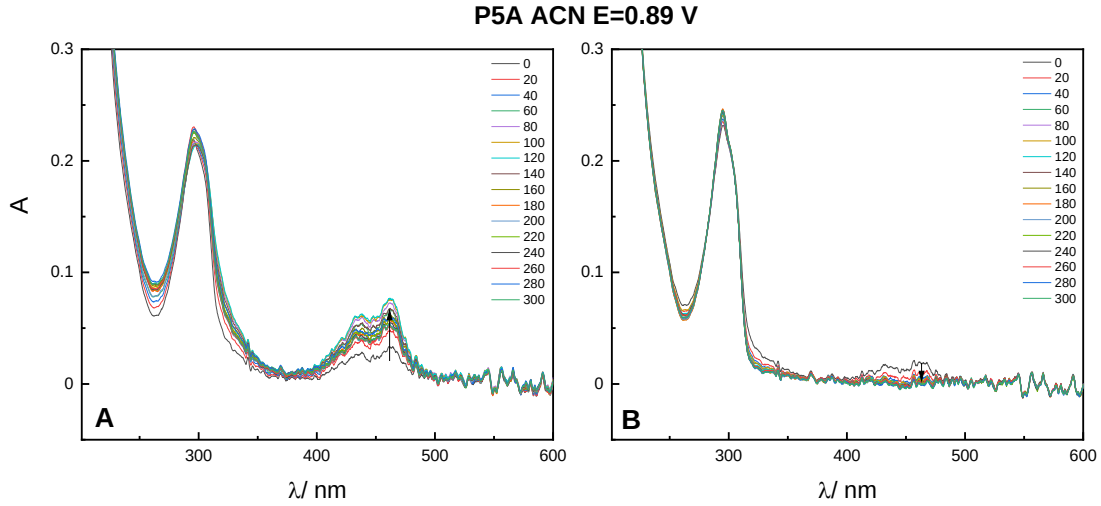
P5A ACN E=0.89 V
A
B
A
λ/ nm
0
20
40
60
80
100
120
140
160
180
200
220
240
260
280
300

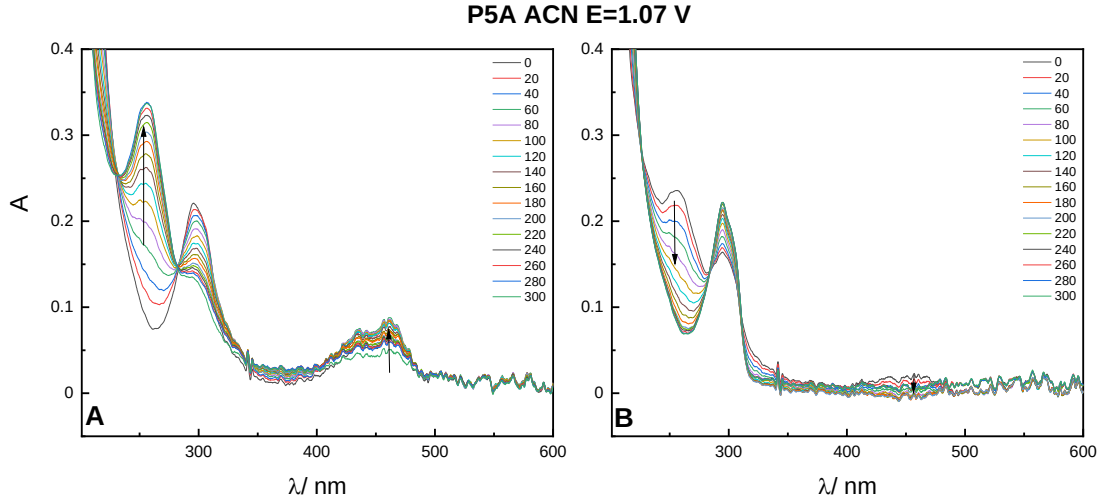
P5A ACN E=1.07 V
A
B
A
λ/ nm
0
20
40
60
80
100
120
140
160
180
200
220
240
260
280
300

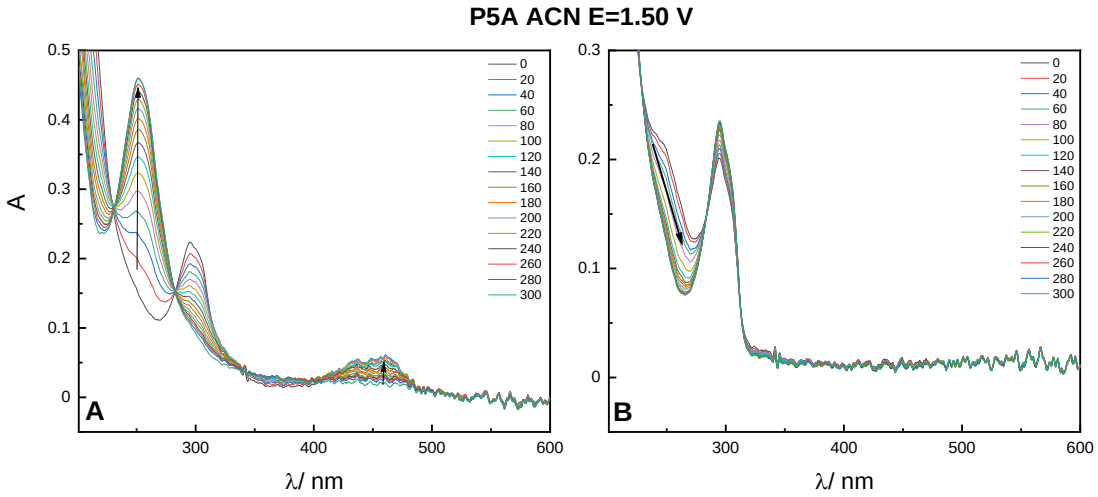

S

SI 3.2 The absorption spectra of **0.1 mM P5A** registered (A) at applied oxidative potential 0.77 V;0.89 V;1.07 V and 1.50 V (B) and after measurements at the applied reductive potential of 0.2 V. Spectra recorded **in ACN** containing **0.1 M TBAHPF** at 22°C.

P5A DCE E=0.89 V

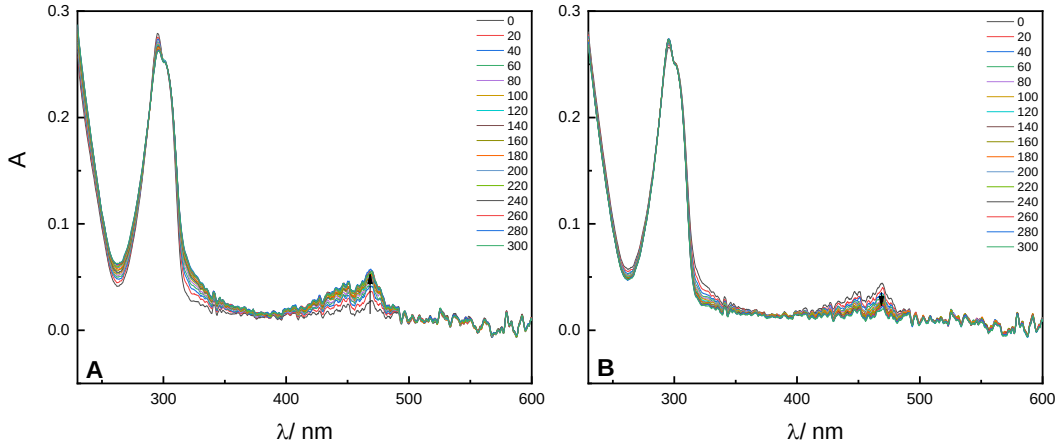

P5A DCE E=1.01 V

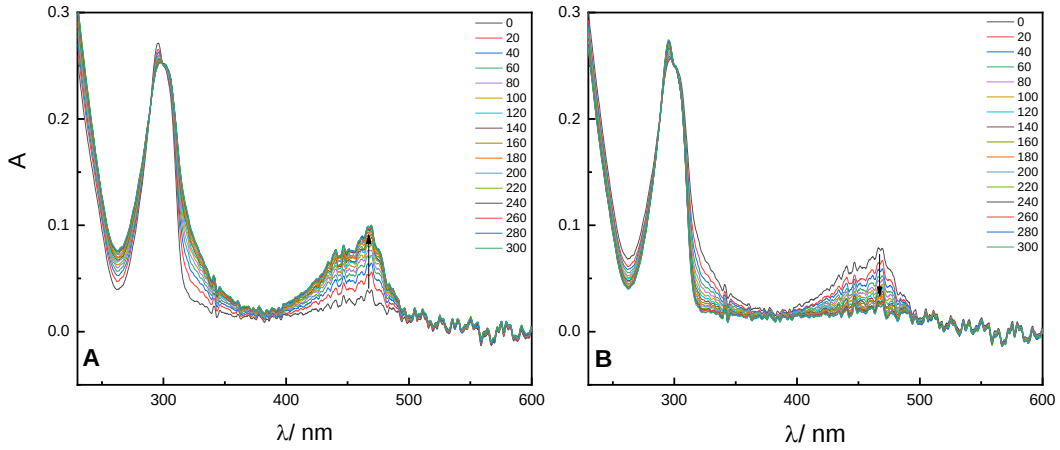

P5A DCE E=1.20 V

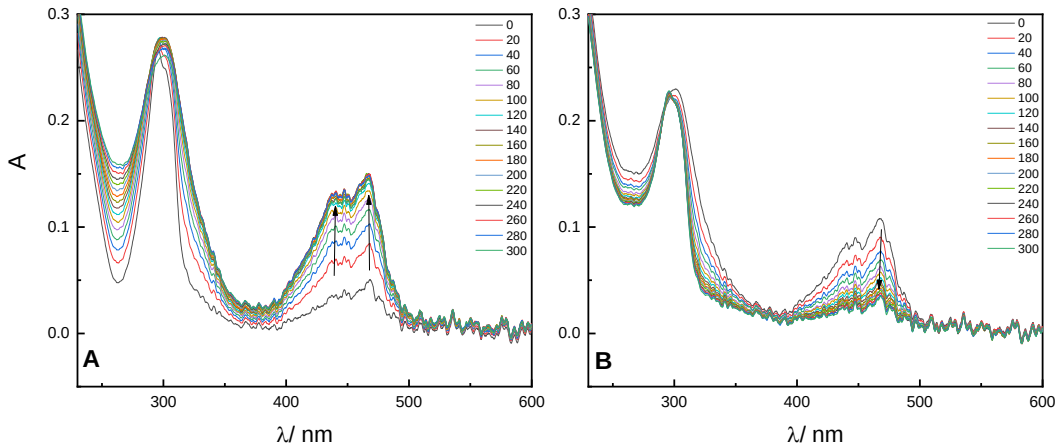

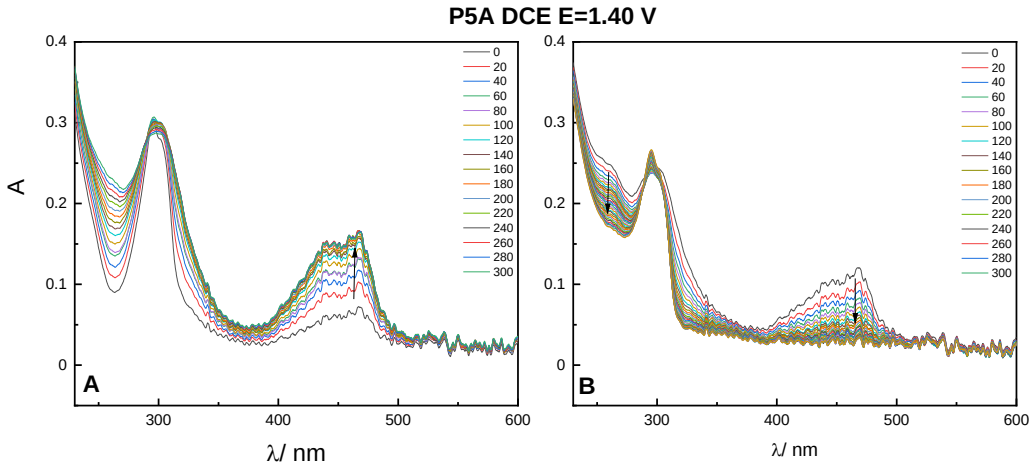

SI 3.3 The absorption spectra of **0.1 mM P5A** registered (A) at applied oxidative potential 0.89 V; 1.01 V; 1.20 V and 1.40 V (B) and after measurements at the applied reductive potential of 0.2 V. Spectra recorded **in DCE** containing **0.1 M TBAHFP** at 22°C.

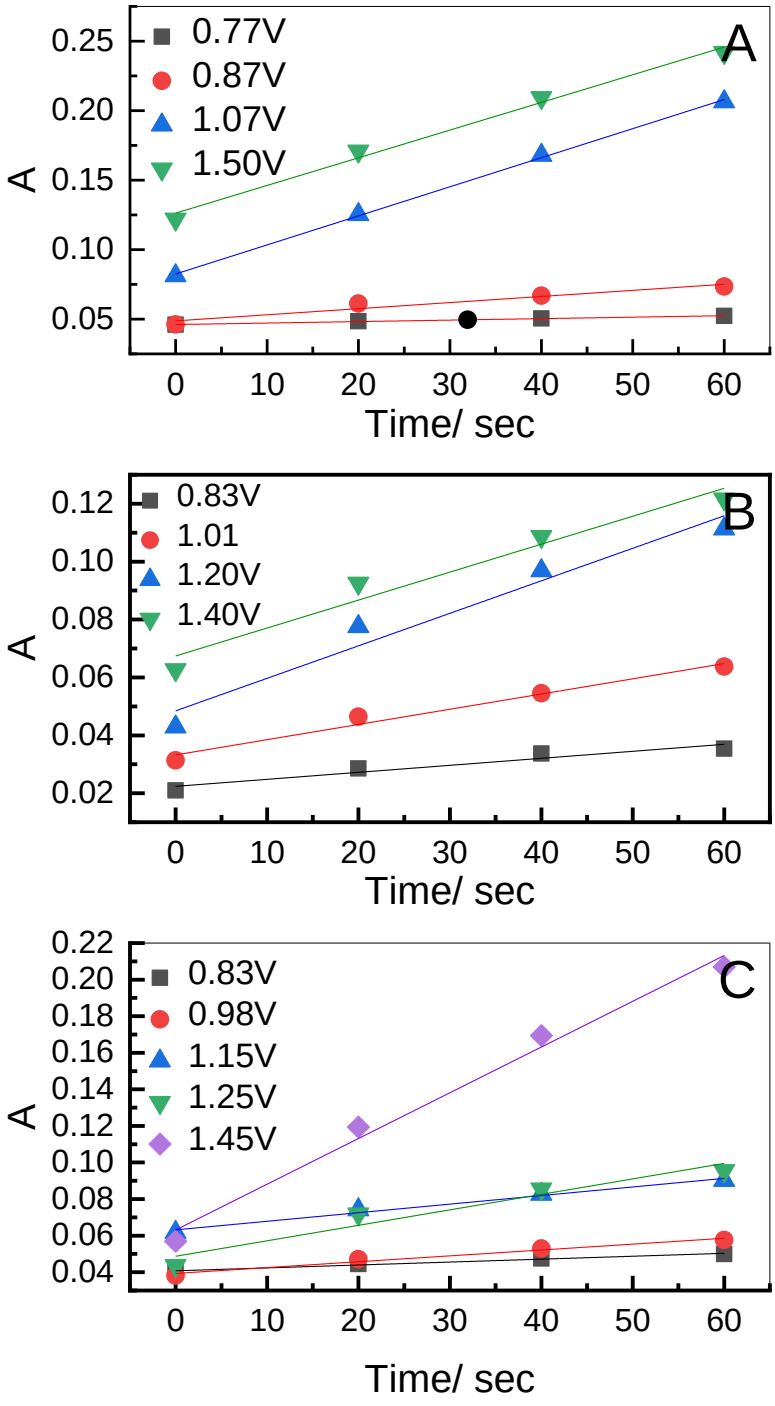

SI 3.4 Changes in the absorption spectra of **0.1 mM P5A** registered during the time at λ= 260 nm. Spectra recorded **in (A) ACN, (B) DCE, (C) DCM** containing **0.1 M TBAHFP** at 22°C.

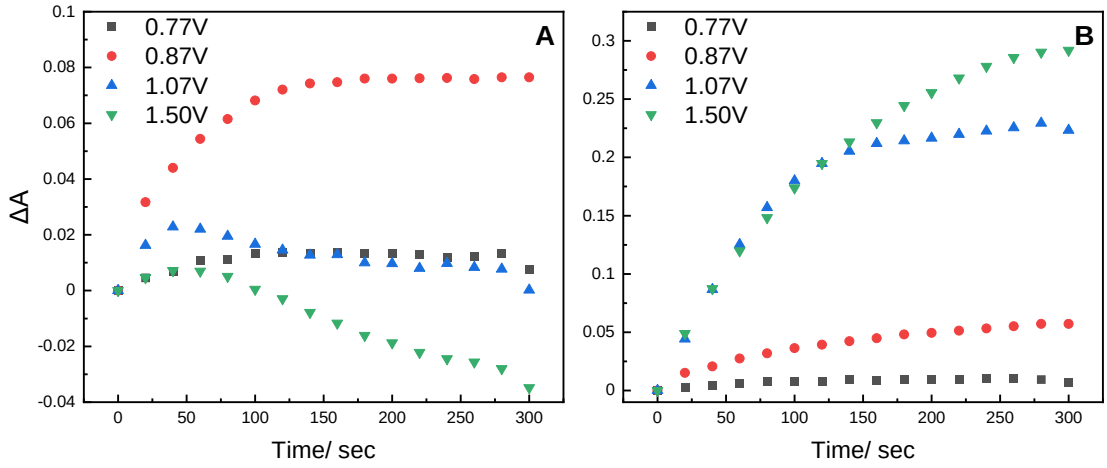

SI 3.5 Changes in the absorption spectra of **0.1 mM P5A** registered during the time for a given wavelength at (A) **λ=464 nm** and (B) **λ= 260 nm**. Spectra recorded **in ACN** containing **0.1 M TBAHFP** at 22℃.

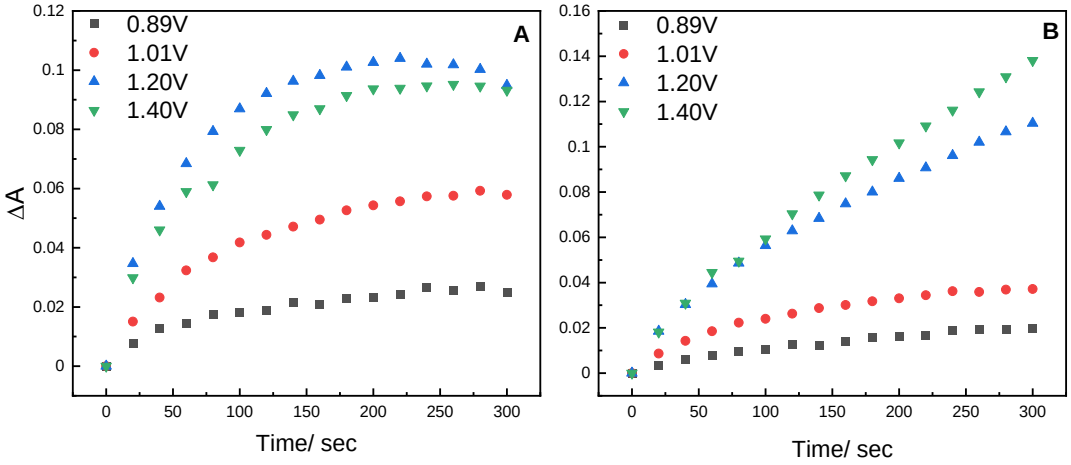

SI 3.6 Changes in the absorption spectra of **0.1 mM P5A** registered during the time for a given wavelength at (A) **λ=464 nm** and (B) **λ= 260 nm**. Spectra recorded **in DCE** containing **0.1 M TBAHFP** at 22℃.

4. Details on NMR

Representative ^{1}H NMR and ^{13}C NMR spectra of the P5A in deuterated chloroform showing a purity of >99%. ^{1}H NMR and ^{13}C NMR were recorded on an Agilent-MR NMR spectrometer (400MHz). All the spectra were internally referenced to residual proton solvent signals. Data for ^{1}H NMR are reported as chemical shift (δ ppm), multiplicity (s = singlet) and integration. Data for ^{13}C NMR are reported as a chemical shift.

^{1}H NMR (400MHz, CDCl3) δ ppm 6.88 (s, 10H), 3.76 (s, 10H), 3.73 (s, 30H)

^{13}C NMR (400 MHz, CDCl3) δ ppm 150.57, 128.31, 113.40, 55.51, 29.38

Bibliography

[1] E.J.F. Dickinson, A.J. Wain, The Butler-Volmer equation in electrochemical theory: Origins, value, and practical application, J. Electroanal. Chem. 872 (2020) 114145. https://doi.org/10.1016/j.jelechem.2020.114145.